

Formation of octahedral FePt nanoparticles by alternate deposition of FePt and MgO

T. Shima^{a)}*Faculty of Engineering, Tohoku-Gakuin University, Tagajyo 985-8537, Japan*

K. Takanashi

Institute for Materials Research, Tohoku University, Sendai 980-8577, Japan

Y. K. Takahashi and K. Hono

National Institute for Materials Science, Tsukuba 305-0047, Japan

(Received 6 June 2005; accepted 22 December 2005; published online 10 February 2006)

Two-dimensional assemblies of octahedral-shaped FePt nanoparticles embedded in a MgO matrix were formed by alternate deposition of FePt and MgO layers on MgO (001) single-crystal substrates with a thermal cycling process. Highly ordered L1₀ structure with the [001] orientation perpendicular to the plane and large coercivity of more than 60 kOe were obtained. Cross-sectional transmission electron microscopy observation revealed that the equilibrium crystal shape of L1₀ ordered FePt particles was octahedral structure due to the anisotropy of the surface energy. The {111} plane shows the minimum surface energy in the L1₀ structure, which is similar to the case of face-centered-cubic structure. © 2006 American Institute of Physics. [DOI: 10.1063/1.2172710]

Recently, nanoscale patterned or particulate magnets are of great interest, since they are believed to be good candidates for future magnetic devices such as next generation ultrahigh-density magnetic storage media and biasing nanomagnets. For any ferromagnetic materials, however, there is a critical grain size where thermal fluctuation becomes dominant at room temperature leading to superparamagnetic behavior. In order to reduce the critical grain size for the superparamagnetic transition, L1₀-ordered FePt alloy with high magnetocrystalline anisotropy ($K_u = 7.0 \times 10^7$ erg/cm³) has attracted much attention, and a lot of studies have focused on the fabrication of L1₀ ordered FePt thin films by conventional deposition techniques^{1–12} and self-organized chemical synthesis.¹³ Several papers also reported on FePt granular films, where FePt nanoparticles were embedded in an oxide matrix, by sputtering¹⁴ and ion implantation¹⁵ techniques. However, highly ordered and highly oriented structure of FePt nanoparticles have not been obtained to date. Previously, we reported that a high coercivity of 70 kOe was successfully achieved at room temperature for FePt particulate films sputtered on MgO (001) substrates.¹ These films had epitaxially grown highly L1₀ ordered structure. In this paper, we demonstrate that the octahedral structure of FePt nanoparticles embedded in MgO matrix can be achieved epitaxially on MgO single crystal substrate by the alternating deposition of FePt and MgO with a thermal cycling process, utilizing the driving force to form the equilibrium crystal shape.¹⁶

The samples in this study were prepared by alternate deposition of FePt and MgO layers onto single crystal MgO (100) substrates through the use of an UHV-compatible dc-sputtering system (base pressure $\sim 5 \times 10^{-10}$ Torr) and an electron beam (EB) evaporation system (base pressure $\sim 1 \times 10^{-9}$ Torr), respectively. The substrates were heated up to 780 °C for FePt layers and cooled down to room tempera-

ture (R.T.) for MgO layers during deposition. The heating rate from R.T. to 780 °C was 20 °C/min and the cooling rate from 780 °C to R.T. was about 10 °C/min. The film construction was [FePt(1.0 nm)/MgO(*t* nm)]₄/FePt(1.0 nm) and the nominal thickness of the MgO layer *t* was varied in the range between 1 and 5 nm, fixing the nominal thickness of FePt at 1 nm. The composition of the films was determined to be Fe₄₈Pt₅₂ by electron probe x-ray microanalysis (EPMA). The structure was characterized by reflection high-energy electron diffraction (RHEED), x-ray diffraction (XRD) and transmission electron microscopy (TEM). The magnetic properties were measured by a vibrating sample magnetometer (VSM) equipped with a superconducting magnet in the field up to 140 kOe at R.T.

XRD patterns for *t* = 1, 2, 3, and 5 nm are shown in Fig. 1. In addition to the fundamental (002) peak, the (001) superlattice peak of the L1₀ phase are clearly observed for *t* = 1 [Fig. 1(a)]. The unlabeled sharp peaks are due to the MgO substrate. No peaks from the other planes of the L1₀

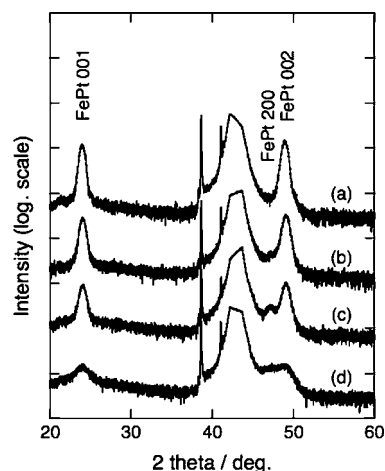


FIG. 1. XRD patterns for [FePt(1.0 nm)/MgO(*t* nm)]₄/FePt(1.0 nm) films with different nominal thicknesses of MgO, *t* = 1 (a), 2 (b), 3 (c), and 5 (d).

^{a)} Author to whom correspondence should be addressed; electronic mail: shima@imr.tohoku.ac.jp

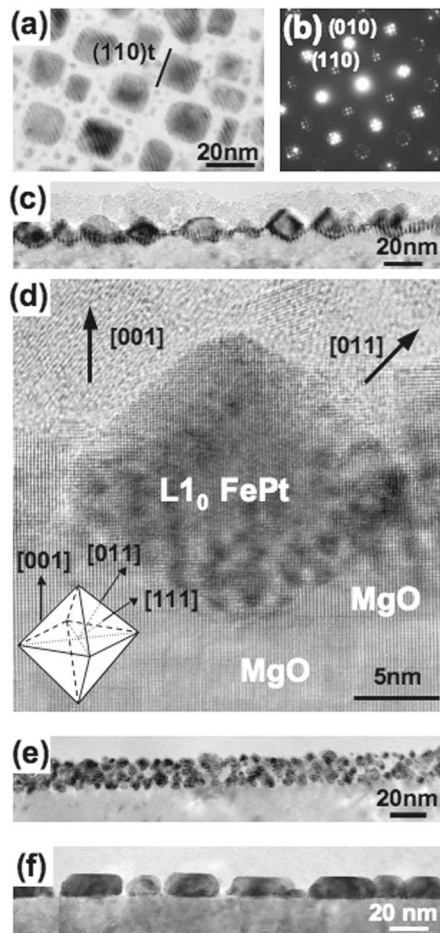


FIG. 2. TEM images for $[\text{FePt}(1.0 \text{ nm})/\text{MgO}(t \text{ nm})]_4/\text{FePt}(1.0 \text{ nm})$ films with $t=1$ and 3 nm and a FePt (5 nm) film directly deposited on a MgO substrate. The in-plane image (a) and the corresponding selected area electron diffraction (ED) pattern (b) for $t=1$; the cross-sectional image for $t=1$ (c), and its high resolution image (d). (Inset denotes schematic illustration of crystal structure.) The cross sectional image for $t=3$ (e), and the cross sectional image for a directly deposited FePt (5 nm) film (f) are shown.

ordered structure are seen. This indicates that the FePt film with the $L1_0$ ordered structure were epitaxially grown on the MgO (001) single crystal substrate, although the sample was prepared by depositing FePt and MgO layers alternately [Fig. 1(a)]. Long range order parameter S was evaluated from the ratio of the integrated intensities of the superlattice peak to the fundamental peak⁹ to be 0.95 ± 0.05 for $t=1$, indicating that a highly ordered $L1_0$ structure was formed. With increasing t , the intensities of both fundamental and superlattice peaks decrease and the (200) peak, which represents the a -plane of the $L1_0$ structure, appear [Figs. 1(b)–1(d)]. In other words, the (001) texture deteriorates with increasing t .

Figure 2 shows transmission electron microscopy (TEM) images for $t=1$ and 3 nm . For comparison, the result for a FePt film with the nominal thickness of 5 nm directly deposited on a MgO substrate is also shown. It is seen in the in-plane image [Fig. 2(a)] that a two-dimensional assembly of FePt nanoparticles with the $\langle 110 \rangle$ terrace of faceted planes are formed for $t=1$ and the typical lateral size of the particles ranges from 10 nm to 20 nm . The selected area diffraction pattern [Fig. 2(b)] indicates the FePt nanoparticles are epitaxially grown with the cube-cube orientation relationship with the MgO substrate, showing the c -axis perpendicular to

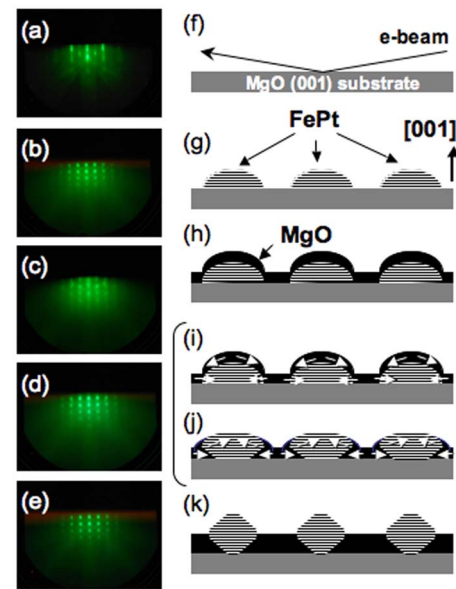


FIG. 3. (Color online) *In situ* RHEED patterns (a–f) for the uppermost layer of the film and illustrations (g–k) of the proposed procedure for the formation of the octahedral-particle assembly. The direction of the incident electron beam for RHEED is $[110]$ on the MgO (001) substrate.

the substrate plane. It is noted that although the samples were prepared by the alternate deposition of FePt and MgO layers, no multilayered structure and no flat interface between the MgO substrate and the film are observed from the cross-sectional image [Fig. 2(c)]. The FePt nanoparticles with octahedral structure are formed and the average heights are almost the same ($\sim 20 \text{ nm}$). The formation of this distinct shape is due to the existence of the anisotropy of the surface energy.¹⁷ The enlarged cross-sectional image [Fig. 2(d)] shows the clear contrast corresponding to the alternating atomic stacking of Fe and Pt layers along the $[001]$ direction of the $L1_0$ structure. The octahedrons are strongly faceted on the $\{111\}$ planes and are grown epitaxially on the MgO single crystal substrate, as shown schematically in the inset. Furthermore, the FePt nanoparticle is formed to be partly buried in the MgO matrix, suggesting that the originally flat MgO surface was zigzagged due to the faceting of the FePt particles. With increasing t , the film shows granular structure consisting of three-dimensionally dispersed FePt nanoparticles with the lateral size in the range from several to 10 nm [Fig. 2(e)]. Figure 2(f) shows the cross-sectional image of a FePt film, a remarkable flat interface between the MgO substrate and the film and the shape of the particles is simple “mesa”-structure.

In situ RHEED observation of the film surface during the alternate deposition of FePt and MgO was performed and it reveals that the reconstruction of the surface occurred. Figure 3 shows the RHEED patterns [Figs. 3(a)–3(e)] and an illustration of the proposed procedure for the formation of the octahedral particle assembly [Figs. 3(f)–3(k)]. The direction of the incident electron beam for RHEED is $[110]$ on the MgO (001) substrate. It is seen that highly ordered FePt particulate structure was formed at high temperature deposition of $T=780 \text{ }^\circ\text{C}$ [Figs. 3(b) and 3(g)] on the MgO substrate [Figs. 3(a) and 3(f)]. Followed by the deposition of a MgO layer at R.T., the pattern turned into a diffused one, showing that the surface of the film was covered with the MgO layer [Figs. 3(c) and 3(h)]. However, with increasing T again, the

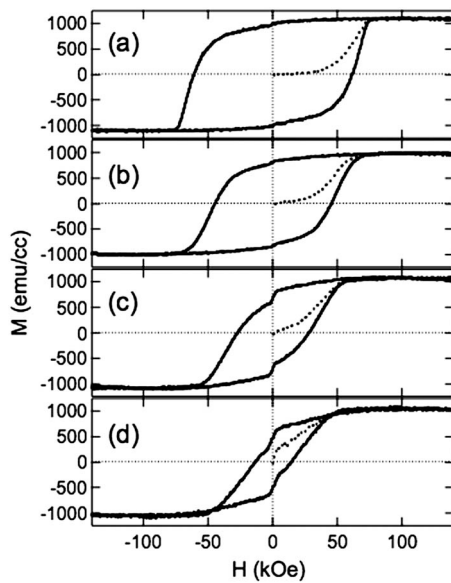


FIG. 4. The magnetization curves for $[\text{FePt}(1.0 \text{ nm})/\text{MgO}(t \text{ nm})]_4/\text{FePt}(1.0 \text{ nm})$ films with $t=1$ (a), 2 (b), 3 (c), and 5 (d). The dotted lines denote initial magnetization curves from the virgin state. Coercivities H_c are 62, 45, 27, and 15 kOe for $t=1, 2, 3,$ and 5 , respectively.

pattern recovered, in other words, it changed again from the diffused into a sharp intense one [Figs. 3(d) and 3(e)]. We consider that by heating the substrate again, the equilibrium crystal shape, i.e., the octahedral shape, is formed when FePt diffuses and comes up to the surface of the MgO layer [Figs. 3(i)–3(k)]. Further deposition of FePt layer at high T promotes the growth of highly ordered octahedral structure. TEM and RHEED observations, in consequence, suggests that the thermal cycling procedure accompanied by the alternate deposition of FePt and MgO contributes to the formation of octahedral structure.

The magnetization measurement reveals that the film with octahedral FePt nanoparticles has high coercivity H_c . The magnetization curves for $t=1, 2, 3,$ and 5 nm are shown in Fig. 4. The dotted lines denote initial magnetization curves from the virgin state. The magnetic field was applied in the perpendicular direction to the film plane. The easy magnetization axis is perpendicular to the film plane for $t=1$ [Fig. 4(a)], which agrees with the XRD result [Fig. 1(a)]. Slow increase of the initial magnetization from the virgin state indicates that FePt nanoparticles have the single domain state. H_c decreases with increasing t , which is also consistent with XRD results [Figs. 1(b)–1(d)] showing the (001) texture of $L1_0$ structure deteriorates with increasing t .

The present study has demonstrated that two-dimensional assemblies of octahedral FePt nanoparticles are formed by the alternate deposition of FePt and MgO layers

with a thermal cycling process. Highly $L1_0$ ordered structure with c -axis orientation perpendicular to the film plane and high H_c of more than 60 kOe have been obtained for octahedral FePt nanoparticles. TEM and *in situ* RHEED observations suggest that the formation of the octahedral structure occurs during the thermal cycling process. The $\{111\}$ plane shows the minimum surface energy of the $L1_0$ structure, which is similar to the case with face centered cubic structure as known from the Wolff construction.¹⁸ The formation of nanostructure using such a kind of equilibrium crystal shape in nanoparticles will be important for the future design of magnetic devices.

This work was partly supported by the Special Coordination Funds for Promoting Science and Technology on “Nanohetero Metallic Materials” from the MEXT. X-ray diffraction measurements were performed at the Laboratory for Advanced Materials, IMR, Tohoku University. High field magnetic measurements were performed at the Centre for Low Temperature Science, Tohoku University. The authors would like to acknowledge Y. Murakami for technical assistance.

- ¹B. M. Lairson, M. R. Viosokay, R. Sinclair, and B. M. Clemens, Appl. Phys. Lett. **62**, 639 (1993).
- ²A. Cebollada, D. Weller, J. Sticht, G. R. Harp, R. F. C. Farrow, R. F. Marks, R. Savoy, and J. C. Scott, Phys. Rev. B **50**, 3419 (1994).
- ³M. Watanabe and M. Homma, Jpn. J. Appl. Phys., Part 1 **35**, L1264 (1996).
- ⁴Y. Ide, T. Goto, K. Kikuchi, K. Watanabe, J. Onagawa, H. Yoshida, and J. M. Cadogan, J. Magn. Magn. Mater. **177–181**, 1245 (1998).
- ⁵T. Suzuki, K. Harada, N. Honda, and K. Ouchi, J. Magn. Magn. Mater. **193**, 85 (1999).
- ⁶D. Ravelosona, C. Chappert, V. Mathet, and H. Bernas, J. Appl. Phys. **87**, 5771 (2000).
- ⁷Y. Endo, N. Kikuchi, O. Kitakami, and Y. Shimada, J. Appl. Phys. **89**, 7065 (2001).
- ⁸Y.-N. Hsu, S. Jeong, D. E. Laughlin, and D. N. Lambeth, J. Appl. Phys. **89**, 7068 (2001).
- ⁹T. Shima, T. Moriguchi, S. Mitani, and K. Takanashi, Appl. Phys. Lett. **80**, 288 (2002).
- ¹⁰T. Shima, K. Takanashi, Y. K. Takahashi, and K. Hono, Appl. Phys. Lett. **81**, 1050 (2002).
- ¹¹T. Seki, T. Shima, K. Takanashi, Y. Takahashi, E. Matsubara, and K. Hono, Appl. Phys. Lett. **82**, 2461 (2003).
- ¹²T. Shima, K. Takanashi, Y. K. Takahashi, and K. Hono, Appl. Phys. Lett. **85**, 2571 (2004).
- ¹³S. Sun, C. B. Murray, D. Weller, L. Folks, and A. Moser, Science **287**, 1989 (2000).
- ¹⁴R. Mukai, T. Umezaki, and A. Tanaka, IEEE Trans. Magn. **39**, 1925 (2003).
- ¹⁵C. W. White, S. P. Withrow, K. D. Sorge, A. Meldrum, J. D. Budai, J. R. Thompson, and L. A. Boatner, J. Appl. Phys. **93**, 5656 (2003).
- ¹⁶A.-C. Shi, Phys. Rev. B **36**, 9068 (1987).
- ¹⁷J. M. Howe, in *Interfaces in Materials: Atomic Structure, Thermodynamics and Kinetics of Solid-Vapor, Solid-Liquid and Solid-Solid Interfaces* (Wiley-Interscience, New York, 1997), p. 63.
- ¹⁸G. Wulff, Z. Kristallogr. Mineral. **34**, 449 (1901).